

# Formulation Development, Optimization and Evaluation of Imipramine Loaded Nano-Structured Lipid Carrier

Rincy Roy, Veinramuthu Sankar\*, Pranav Ragavendra

Department of Pharmaceutics, PSG College of Pharmacy, Coimbatore, (Affiliated to The Tamil Nadu Dr MGR Medical University, Chennai), Tamil Nadu, INDIA.

## ABSTRACT

**Background:** Nano-structure Lipid Carriers (NLCs) are small spheres extending in scale from 10 to 1000 nanometres comprised of biocompatible and biodegradable lipids. These spheres can encapsulate both hydrophilic and lipophilic drugs, preserving them from degradation and increasing their distribution to the intended place in the body. Imipramine, a tricyclic antidepressant, has been investigated in hamster model at 5-10 mg/kg for experimental leishmaniasis. The goal of this research is to develop Imipramine in a nano-structured lipid carrier formulation for targeting macrophage cells. **Materials and Methods:** Imipramine-loaded NLCs were created employing Glyceryl Monostearate (GMS) as the solid lipid constituent alongside oleic acid as the liquid lipid, while tween80 acted as the surfactant. The process of hot homogenization was employed to prepare the NLCs. The formulation was optimized using  $2^3$  factorial designs using design expert software. The optimised formulation was further used for the preparation of mannose functionalized imipramine-loaded NLCs. **Results:** The IMP-NLC opt and M-NLC show a globule size of  $348.5 \pm 0.81$  nm and  $459.4 \pm 0.28$  nm with encapsulation efficiency of  $61.6 \pm 0.326\%$  and  $64.48 \pm 0.408\%$ , respectively. The drug release *in vitro* demonstrates a dual-phase pattern, featuring an early rapid sudden release followed by a gradual and slower release. The surface morphology, drug release kinetics and stability were also used to characterize the prepared NLCs. **Conclusion:** This study concludes that nanostructured lipid carriers demonstrate considerable encapsulation efficiency, release and stability for further pre-clinical investigation.

**Keywords:** Imipramine, Nanostructure lipid carrier,  $2^3$  factorial design, Particle size, Encapsulation efficiency.

## Correspondence:

**Dr. V. Sankar**

Professor, Department of Pharmaceutics,  
PSG College of Pharmacy, Coimbatore,  
Tamil Nadu, INDIA.  
Email: veinramuthu@gmail.com

**Received:** 25-03-2024;

**Revised:** 15-05-2024;

**Accepted:** 16-05-2024.

## INTRODUCTION

Among nano-drug delivery systems, lipid-based delivery has gained immense popularity. Nano-lipid carriers, representing the next generation of nanoparticles constructed from lipids, have emerged as a hopeful platform for drug delivery, addressing limitations associated with conventional drug therapy.<sup>1</sup> Nanostructured Lipid Carriers (NLCs) are binary systems composed of solid-liquid blends, resulting in a less ordered lipidic core. This imperfect internal arrangement enables better drug accommodation, addressing the low drug payload issue observed in Solid Lipid Nanoparticles (SLN).<sup>2</sup> NLCs offer numerous advantages compared to SLNs, including their ability to accommodate a greater variety of drugs, lower lipid content and enhanced drug entrapment while minimizing drug loss during storage.<sup>3</sup>

Macrophages in our immune system, also known as eating cells, play a double-edged second role in leishmaniasis infection. They can destroy the ingested parasite but can also be exploited as a safe haven for leishmania to multiply.<sup>4</sup>

The current treatment options for leishmaniasis include pentavalent antimonial as first-line treatments in many regions, pentavalent antimonial such as sodium stibogluconate or meglumine antimoniate.<sup>5</sup> Amphotericin deoxycholate, pentamidine and miltefosine as second-line treatments. Even though pentavalent antimonial are the primary choice for treating leishmaniasis, resistance is prevalent. Amphotericin B is effective but has several side effects and alternate drugs like miltefosine and paromomycin face issues related to resistance and toxicity, like nephrotoxicity.<sup>6</sup>

In previous studies, Imipramine, a tricyclic anti-depressant, has been proven to be exceptionally potent against antimony-resistant clinical *Leishmania donovani* (LD) isolate in the *in vivo* and *in vitro*, as evidenced by an experimental hamster model with a full 28-day oral treatment. The study suggests that imipramine works by generating harmful molecules such as Reactive Oxygen Species and Nitric Oxide (ROS and NO) that kill the parasite within the



DOI: 10.5530/jyp.2024.16.68

### Copyright Information :

Copyright Author (s) 2024 Distributed under  
Creative Commons CC-BY 4.0

Publishing Partner : EManuscript Tech. [www.emanuscript.in]

infected cells and also modulates histone deacetylase II, leading to a strange immune response in macrophages.<sup>7</sup>

Macrophage tends to express many carbohydrate receptors, such as mannose, galactose, fructose and fucose. Particularly, the presence of mannose receptors exclusively on macrophages has been harnessed in the development of effective drug carriers specially targeted to those immune cells.<sup>8</sup>

The goal of the ongoing investigation was to design and formulate NLCs utilizing combinations of solid and liquid lipid mixtures employing the hot homogenization method to deliver imipramine to macrophage cells present in the reticuloendothelial system, i.e., the liver and spleen.

## MATERIALS AND METHODS

### Materials

Imipramine Hydrochloride was gifted from R.L. Fine chemical Karnataka, Bangalore. Glyceryl Monostearate (GMS) was acquired from Loba chemie Pvt. Ltd., Oleic Acid (OA) were obtained from Rankem Laboratory Reagent and Tween 80 were purchased from Fischer Scientific. D-mannose were obtained from Loba chemie Pvt. Ltd., Potassium dihydrogen phosphate and sodium hydroxide supplied from Nice Chemicals Pvt. Ltd.

### Methods

#### *Optimization of Imipramine loaded Nano-structured Lipid Carrier*

In nanoparticle-based formulation optimization, systematic experiment planning is crucial to ensure efficiency and accuracy. A 2<sup>3</sup> factorial experimental design was employed to investigate the impact of three independent variables at two levels each on dependent variables. This design facilitated the examination of all possible combinations, aiding in assessing primary components and interaction effects. The independent factors included total lipid quantity, homogenization rate and concentration of surfactant, while dependent factors encompassed particle size dimension, encapsulation efficiency and zeta potential. Design Expert software version 13.0 (State Ease) was utilized for analysis, for the selection of the optimized batch based on predefined criteria such as maintaining factors within specified ranges, minimizing particle size, maximizing encapsulation efficiency and zeta potential. The desirability factor, aiming for values close to 1, guided the selection process. The details of the design are outlined in Table 1.

#### **Preparation of Imipramine loaded NLCs**

The NLCs were produced utilizing the heat homogenization method, with a ratio of solid lipid to liquid lipid set at 70:30 in which Glyceryl monostearate as solid lipid and oleic acid as liquid lipid. The lipids were heated to 70°C until melted, following which the medication was introduced into the transparent oil phase.

The aqueous phase, which contained double-distilled water and a surfactant (Tween 80), was transferred to the oily phase and stirred in a magnetic stirrer to form a primary emulsion. This was then subjected to high shear homogenization (Omni GLH 850) at variable speed for 15 min, resulting in the formation of a nano emulsion. The nano emulsion was allowed to settle and stored at the ambient temperature.<sup>9</sup>

#### **Formulation of mannose functionalized NLCs**

The process of applying a mannose coating to uncoated NLCs was carried out using an adapted approach based on a previously documented method.<sup>10</sup> Initially, a solution with a concentration 50 milli-molar mannose containing solution was dissolved in acetate buffer at pH 4 and added to NLC suspension with its surface modified using stearyl amine. The blend was continuously stirred gently for 48 hr.<sup>11</sup> The mannose-coated nanoparticles were filtered using haemodialysis membranes with a nominal molecular weight threshold of 10-12 kDa for 1 hr.

### Characterization

#### *Particle size, PDI determination*

The particle diameter was obtained using main scattering of Dynamic Light (DLS) using a zeta sizer (Malvern Zeta Sizer ZS90) at a scattering angle of 90°. Before doing evaluations, the samples were diluted with distilled water. The Z-average size of the particle and the Polydispersity Index (PDI) were determined to quantify the spread of the particle size dimension.

#### **Zeta potential measurements**

The zeta potential of the particles was determined by particle movement under an electric field (electrophoretic mobility) using a Malvern Zeta Sizer (ZS90). Before measuring, the samples were diluted with water. The samples were analysed in triple.

#### **Encapsulation Efficiency**

Imipramine entrapment within the lipid carrier was assessed by centrifuging 2 mL of the NLCs dispersion at 10000 rpm and subsequently collecting the supernatant. The supernatant is filtered through 0.25 µ filter and absorbance was checked using UV-visible spectrophotometer at 251 nm. The encapsulation efficiency has been determined applying the formula provided below.

$$\% EE = \frac{W_1 - W_2}{W_1} \times 100$$

Where, W1-total weight of drug added in the NLC formulation, W2-drug present in the supernatant.

#### **Fourier Transform Infrared Spectroscopy (FT-IR) Analysis**

FTIR analysis was used for drug and excipient analysis and compatibility studies. Pure drugs, solid lipids, liquid lipids and

physical mixtures are analyzed using the KBR pellet method. The investigation was conducted using Shimadzu FTIR 8400 S. The samples were compressed against a hydraulic press to form discs. The wavelength ranges were selected between 400 and 4000  $\text{cm}^{-1}$ .

## Surface morphology Characterization

### Atomic-Force Microscopy (AFM) measurements

AFM, a surface analysis method, allows high-resolution imaging of micro/nanostructured coatings in air or liquid. NLC dispersion was diluted, applied to a slide and dried naturally. The dried film was analyzed using AFM NT-MDT model, NTEGRA, Russia.

### Phase-contrast Microscopy

The structure of NLCs dispersion was examined using a phase-contrast lens and a Nikon Leica inverted phase contrast microscope. The sample was mounted on a slide and imaged using Leica software, allowing for the determination of the formulation's shape.

### In vitro release analysis

*In vitro* release studies were conducted on optimized NLC formulations, followed by the generation of mannosylated coated NLCs using the dialysis sac technique. The molecular threshold for dialysis was set at 10-12 kilo Dalton, using a phosphate buffer with pH 6.8 for an 8 hr duration. A volume equivalent to 1 mg of drug from the NLC formulation was placed in a dialysis membrane and immersed in 200 mL of phosphate buffer at  $37 \pm 0.5^\circ\text{C}$  with agitation at 100 rpm. Dialysis solution samples were collected at 0.5, 1, 2, 3, 4, 5, 6, 7 and 8 hr intervals, maintaining sink conditions by replenishing buffer volume. The formulation will be examined using UV spectroscopy at 251 nanometres.

### Kinetics model studies

Drug release delivery data obtained for optimized NLC formulations (IMP-NLC opt) and mannosylated NLCs were fitted to a mathematical model using a DD solver. The *in vitro* study data were subjected to various kinetic models. A comprehensive range of kinetic models, comprising zero-order, first-order, Higuchi's, Hixson-Crowell, Korsmeyer-Peppas, alongside the Weibull method, were utilized to investigate the dynamics and mechanisms underlying drug release.<sup>12</sup> The most appropriate fitting was chosen based on the highest level of regression ( $r^2$ ) correlation value.

### Statistical Data Analysis

Analysis of data was carried out utilizing GraphPad Prism software version 10 for statistical purposes. The results were examined in threefold and shown as mean  $\pm$  standard deviation, for independent experiments. The findings were deemed significant at a threshold of  $p < 0.005$  through the application of 'one-way ANOVA' and 'one sample student's *t*-test'.

## RESULTS

### Optimization of Imipramine containing NLCs

Design Expert® software version 13.0 (State Ease) was used to optimize formulations with eight variations based on lipid quantity, homogenization rate and surfactant concentration. Responses included particle size, encapsulation efficiency and zeta potential which was indicated in Table 2. Statistical analysis, including ANOVA and model summary, ensured the model's accuracy. Results indicated strong alignment with the dataset, confirming a robust fit. Summary statistics and ANOVA analysis results are provided in Tables 3 and 4.

### Independent factors effect on particle size response

The polynomial equation relates three factors (A, B, C) to the particle size of imipramine-loaded NLC dispersions, with sizes ranging from 330 to 693 nm with lowest particle size for formulation 7 and highest for formulation 5 which was given below,

$$\text{Particle size} = +423.54 + 67.06 B - 81.66 C - 72.09 BC$$

A-Total lipid quantity, B-Homogenization rate, C-Concentration of surfactant.

Here, the positive and negative values indicate favourable and unfavourable effects on size of the Particle (PS), respectively. Homogenization speed positively impacts Particle Size (PS), while higher surfactant concentration leads to decreased particle size, in line with previous research.<sup>13</sup> This suggests that surfactant reduces interfacial tension between phases, enhancing emulsification efficiency.

### Independent factors effect on encapsulation efficiency response

According to Table 2, the entrapment efficiency percentage varies between 58.83% and 71.57%, with the highest entrapment efficiency observed in the F3 formulation and the lowest value for the F2 formulation which were indicated in Table 2. The influence of different variables, such as is represented by the polynomial equation given below.

$$\text{Entrapment efficiency} = +66.55 - 2.19A + 1.94 B + 2.31BC + 1.26ABC,$$

where

A-Total lipid quantity, B-Homogenization rate, C-Concentration of surfactant.

The data in Table 2 underscores the significant influence of lipid quantity on entrapment efficiency, with higher lipid concentrations leading to reduced encapsulation efficiency, possibly due to lipid matrix instabilities which contradicts with previous findings.<sup>14</sup> Additionally, the interaction between

factors ABC and BC suggests a synergistic effect, indicating that surfactants may enhance encapsulation efficiency by improving solubilization. Moreover, higher homogenization speeds correlate with increased encapsulation efficiency, likely attributed to smaller particle sizes.

### Independent factors effect on zeta potential response

Zeta potential is critical for NLC formulations, affecting their stability and performance with values ranging from -2.9 to -19.6. According to Table 2 the highest value was found in F2 and the lowest in F6. A polynomial equation describes how lipid amount, homogenization rate and surfactant concentration impact zeta potential was indicated below

$$\text{Zeta potential} = -9.54 + 1.10A + 3.96B - 1.60C + 1.10AB - 1.70AC,$$

where

A-Total lipid quantity, B-Homogenization rate, C-Concentration of surfactant.

Here, the total quality of lipid and concentration of surfactant exert a negative effect on zeta potential, while the combination of the total amount of lipid and homogenization rate produces a positive effect on zeta potential. The negative influence on zeta potential is connected with the presence of lipids with negative charge and the comparatively minimal impact on zeta potential is owing to the employment of a non-ionic surfactant and the drug's positive charge.<sup>15</sup>

The optimal formulation for imipramine-loaded Nanostructured Lipid Carriers (NLCs) was determined using Design Expert software. It comprised total lipid quantity (594 mg), homogenization rate (10008 rpm) and surfactant concentration (1.9%), achieving desired outcomes with a desirability value of 1. The formulation resulted in particle size of  $348 \pm 0.81$  nm, encapsulation efficiency of  $61.6 \pm 0.326\%$  and zeta potential of  $-12 \pm 1.15$  mV. The interplay between dependant and independent variables were analyzed through response surface plots given in Figure 1.

### Characterization of IMP-NLC opt and M-NLC

#### Particle size, PDI determination

The mean particle sizes for Optimized IMP-NLCs (IMP-NLC opt) and mannosylated NLCs (M-NLC) were determined using the Malvern zeta sizer, resulting in values of  $348.5 \pm 0.81$  nm and  $459.4 \pm 0.28$  nm, respectively. The Polydispersity Index (PDI), used to assess the homogeneity of the particle size in the formulation, was found to be  $0.406 \pm 0.002$  for optimized NLCs (IMP-NLC opt) and  $0.394 \pm 0.012$  for mannosylated NLC (M-NLC) which were depicted in Figure 2.

### Zeta potential measurement

Zeta potential measurements showed  $-12 \pm 1.15$  mV for IMP-NLC opt and  $-39.7 \pm 0.75$  mV for M-NLC, indicating electrostatic repulsion between particles. Figures 3 display the zeta potential graphs for both formulations, highlighting the difference in surface potential, with M-NLC having a more negative zeta potential.

### Encapsulation Efficiency

The encapsulation efficiency for IMP-NLC opt was identified to be  $61.6 \pm 0.326\%$ , while M-NLC exhibited an encapsulation efficiency of  $64.48 \pm 0.408\%$ . Both were significant ( $p < 0.005$ ) based on a one-sample t-test, indicating their capacity to incorporate the drug into the lipid carrier.

### Surface morphology

#### Phase contrast microscopy

The phase contrast microscope image depicts spherical shape NLCs for both IMP-NLC opt and mannosylated NLC. The image all show the rigidity of NLCs dispersion. The IMP-NLC opt and M-NLC are shown in Figure 4.

### Atomic force microscopy

In Figure 5, the 3D surface morphology of IMP-NLC and M-NLC. IMP-NLC exhibits an average height of 246.4 nm with a roughness of 19.1308, along with skewness and kurtosis values of 0.4992237 and 1.46774, respectively. In contrast, M-NLC has an average height of 322.771 nm and a roughness of 26.1169, with skewness and kurtosis values of 1.09595 and 3.68718, respectively.

### Fourier Transform Infrared Spectroscopy (FT-IR) Analysis

Figure 6 represents FTIR analysis of the drug-excipients interaction. In the physical mixture, characteristic peaks at  $2882.81 \text{ cm}^{-1}$  (C-H stretching),  $1244.47 \text{ cm}^{-1}$  (C-N stretching),  $1731.03 \text{ cm}^{-1}$  (C=O stretching) and  $1467.88 \text{ cm}^{-1}$  (C-H bending) confirm imipramine hydrochloride, glyceryl monostearate and oleic acid presence.

M-NLC's spectrum reveals mannose conjugation via a Schiff base (R-CH=N-R bond), evidenced by a peak at  $1634.73 \text{ cm}^{-1}$ .

**Table 1: Different levels of independent fact.**

| Independent factors                | Level |       |
|------------------------------------|-------|-------|
|                                    | High  | Low   |
| A: Total quantity of lipids (mg)   | 400   | 600   |
| B: Homogenization Rate(rpm)        | 10000 | 12000 |
| C: Concentration of surfactant (%) | 1.5   | 2.5   |



## In vitro release analysis

The drug's *in vitro* release investigations were done utilising the dialysis diffusion bag technique with a pH 6.8 phosphate buffer. The release at the end of 8 hr demonstrated a percentage release of  $47.94\% \pm 2.38$  for IMP-NLC opt and  $28.8\% \pm 1.50$  for M-NLC. Among the eight formulations, the maximum percentage release was observed for the F3 formulation at 58.42%, while the minimum percentage release was noted for the F2 formulation at 29%. The statistical difference was found to be significant using a one-sample t-test ( $p < 0.001$ ) for both IMP-NLC opt and M-NLC. Comparison of the eight NLC formulations was found to be significant using one-way ANOVA ( $p \leq 0.0001$ ) where represented in Figure 7.

## Kinetics model studies

The release data for IMP-NLC and M-NLC formulations were analyzed using various mathematical models to determine the drug release mechanism which was indicated in Table 5. For IMP-NLC, the Weibull model provided the best fit with an  $R^2$  value of 0.9941, indicating Fickian diffusion as the primary transport mechanism. A Weibull value " $\beta$ " smaller than 0.75 suggests Fickian diffusion. On the other hand, M-NLC exhibited the highest  $R^2$  value of 0.9467 with the korsmeyer-peppas kinetic model, suggesting anomalous or non-Fickian diffusion characterized by an 'n' value of 0.516. Both formulations followed first-order release kinetics, with  $R^2$  values of 0.8381 and 0.8234 respectively.

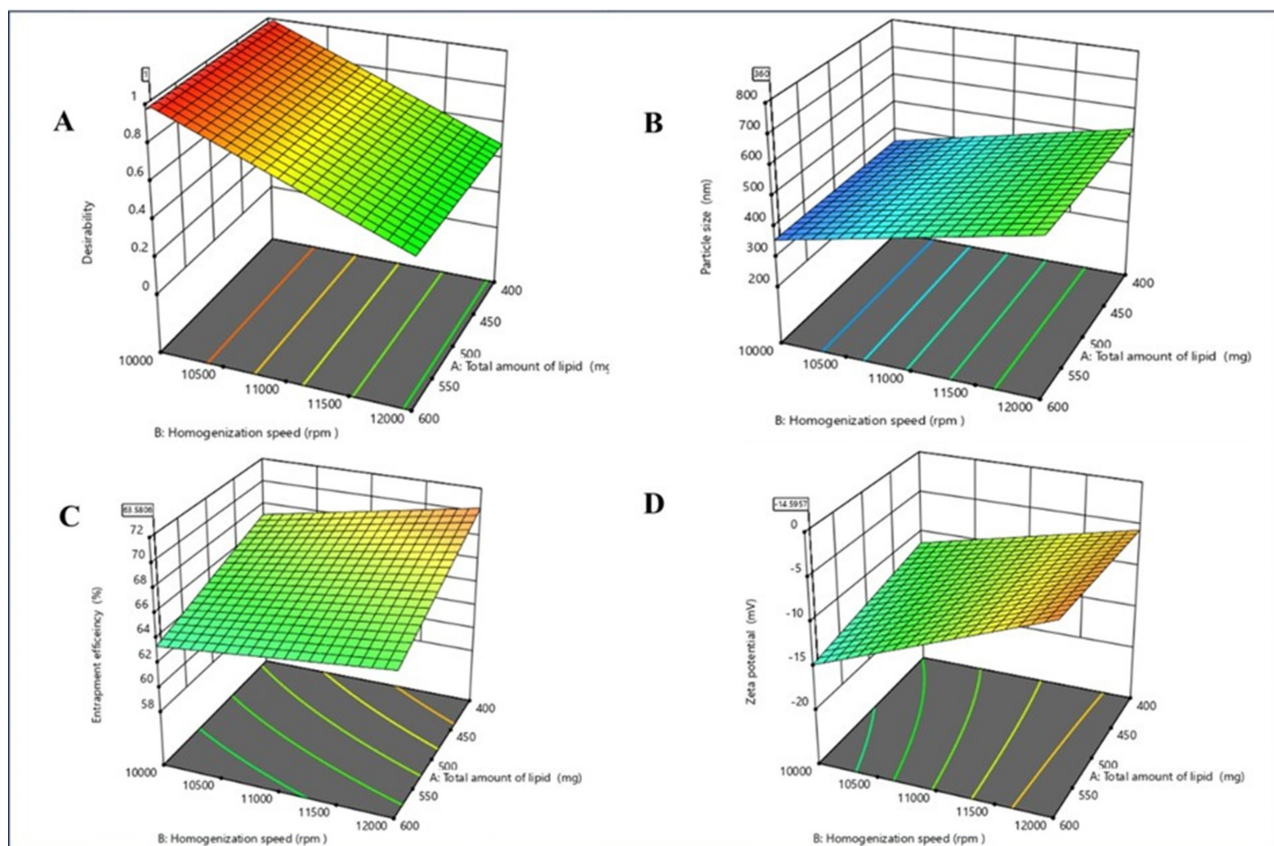


**Figure 1:** Response surface plot (3D plot) on A) Desirability and responses B) Particle size (PS) C) Encapsulation efficiency D) Zeta potential.

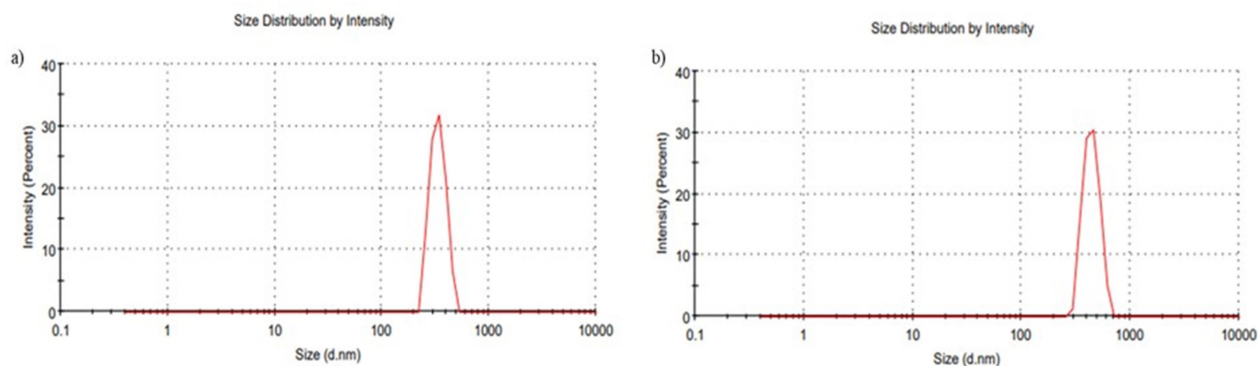


**Figure 2:** Particle size of a) Imp-NLC opt b) M-NLC.

## DISCUSSION

The implementation of imipramine-loaded Nanostructured Carriers (NLC) has demonstrated as an effective method for drug delivery in to macrophages. Statistical tools,  $2^3$  factorial designs, were utilized to assess the effects of total lipid quantity (A), homogenization rate (B) and surfactant Concentration (C) on response particle size dimension (Y1), encapsulation

efficiency (Y2) and zeta potential (Y3). Polynomial equations were derived to analyze the significant impacts of these factors on the responses. Figure 1 illustrates response surface graphs depicting the interactions among these variables and their effects on the responses.

Particle size distribution and PDI of formulations were analyzed using the Malvern Zeta Sizer. Results revealed that the mean

**Table2:  $2^3$  factorial designs for Imipramine -loaded NLC.**

| Formulation Code | Factors                      |                              |                                    | Response           |                              |                     |
|------------------|------------------------------|------------------------------|------------------------------------|--------------------|------------------------------|---------------------|
|                  | A: Total lipid quantity (mg) | B: Homogenization rate (rpm) | C: Concentration of surfactant (%) | Particle Size (nm) | Encapsulation efficiency (%) | Zeta Potential (mV) |
| F1               | 400                          | 10000                        | 1.5                                | 396.6              | 66.6                         | -11.8               |
| F2               | 600                          | 10000                        | 1.5                                | 362.9              | 58.83                        | -19.6               |
| F3               | 400                          | 12000                        | 1.5                                | 343.1              | 71.57                        | -5.28               |
| F4               | 600                          | 12000                        | 1.5                                | 335.5              | 68.02                        | -11.2               |
| F5               | 400                          | 10000                        | 2.5                                | 693.5              | 70.38                        | -5.8                |
| F6               | 600                          | 10000                        | 2.5                                | 595.2              | 62.74                        | -2.9                |
| F7               | 400                          | 12000                        | 2.5                                | 330.6              | 69.27                        | -8.27               |
| F8               | 600                          | 12000                        | 2.5                                | 330.9              | 65                           | -11.4               |

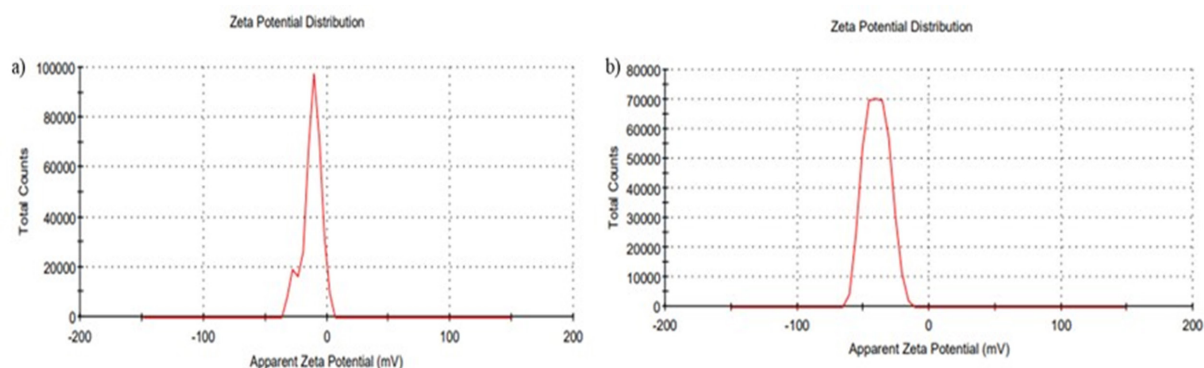


**Figure 3:** Zeta Potential of a) IMP-NLC opt b) M-NLC.

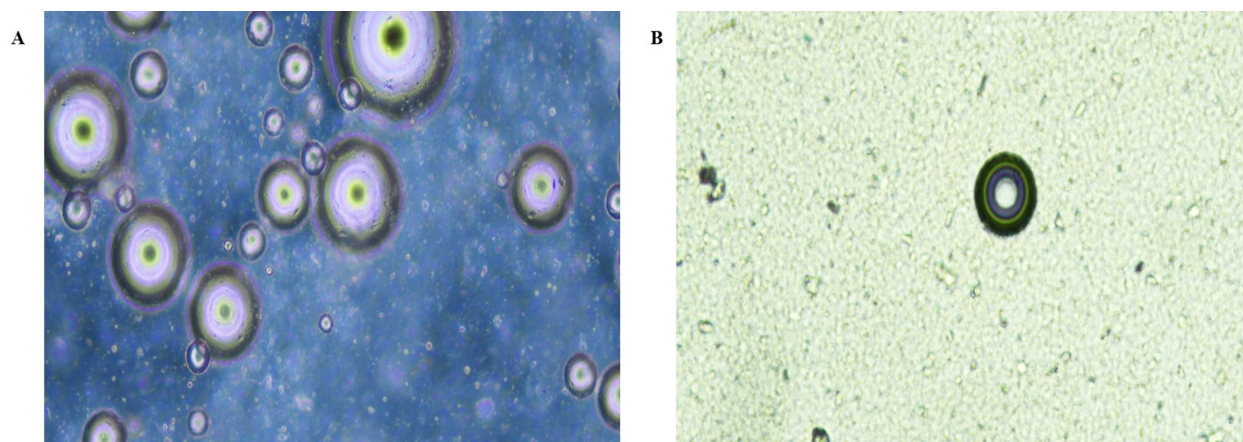


**Figure 4:** Phase contrast images of A) IMP-NLC opt B) M-NLC at 10x.

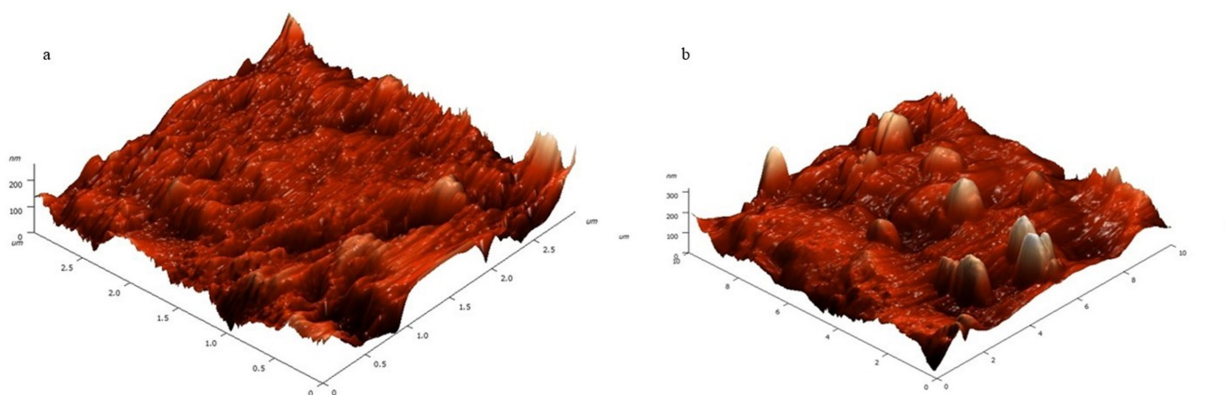


**Figure 5:** AFM 3D images of a) IMP-NLC opt and b) M-NLC for morphological determination.

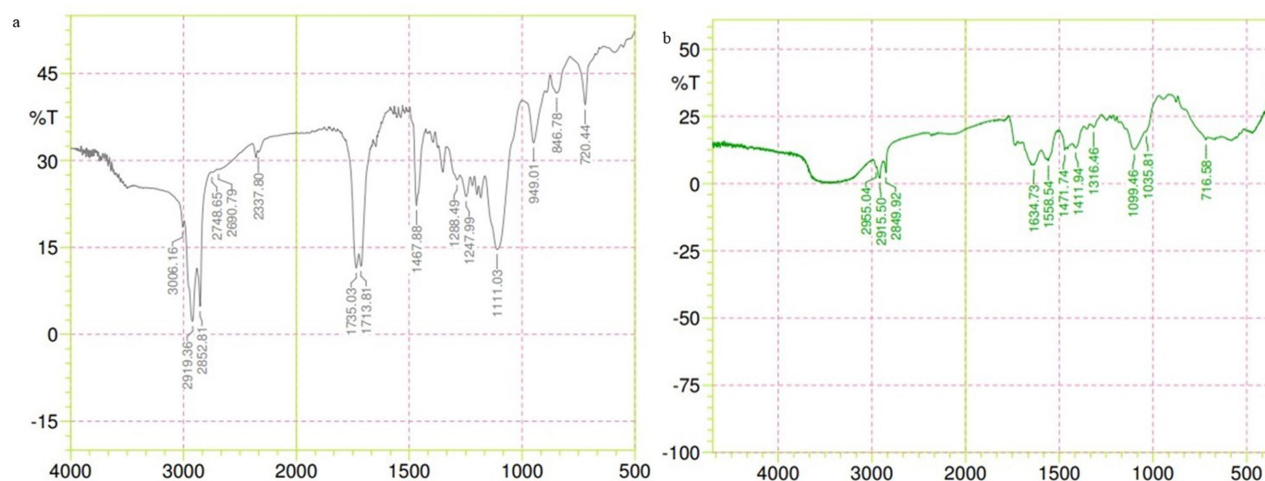


**Figure 6:** FTIR Spectrum OF a) Physical mixture b) M-NLC.

**Table 3: Model statistics for the responses.**

| Response              | R <sup>2</sup> | Adjusted R <sup>2</sup> | Predicted R <sup>2</sup> | Adequate precision |
|-----------------------|----------------|-------------------------|--------------------------|--------------------|
| Particle size         | 0.9473         | 0.9077                  | 0.7890                   | 10.1878            |
| Entrapment efficiency | 0.9846         | 0.9646                  | 0.8921                   | 20.198             |
| Zeta potential        | 0.9914         | 0.9698                  | 0.8620                   | 21.3196            |

**Table 4: ANOVA analysis for responses.**

| Response              | Sum of Square | Mean Square | F-value | p-value | Status      |
|-----------------------|---------------|-------------|---------|---------|-------------|
| Particle size         | 1.309         | 43634       | 23.95   | 0.0051  | Significant |
| Entrapment efficiency | 124.04        | 31.01       | 60.27   | 0.0044  | Significant |
| Zeta potential        | 188.14        | 37.63       | 45.99   | 0.0750  | Significant |

**Table 5: Drug release profile kinetics of IMP-NLC opt and M-NLC showing R<sup>2</sup> value.**

| Formulation Name | Zero order | First order | Higuchi's | Korsmeyer Peppas | Hixson Crowell | Weibull |
|------------------|------------|-------------|-----------|------------------|----------------|---------|
| IMP-NLC opt      | 0.7109     | 0.8381      | 0.9863    | 0.9889           | 0.8015         | 0.9941  |
| M-NLC            | 0.7834     | 0.8234      | 0.9467    | 0.9469           | 0.8112         | 0.8112  |



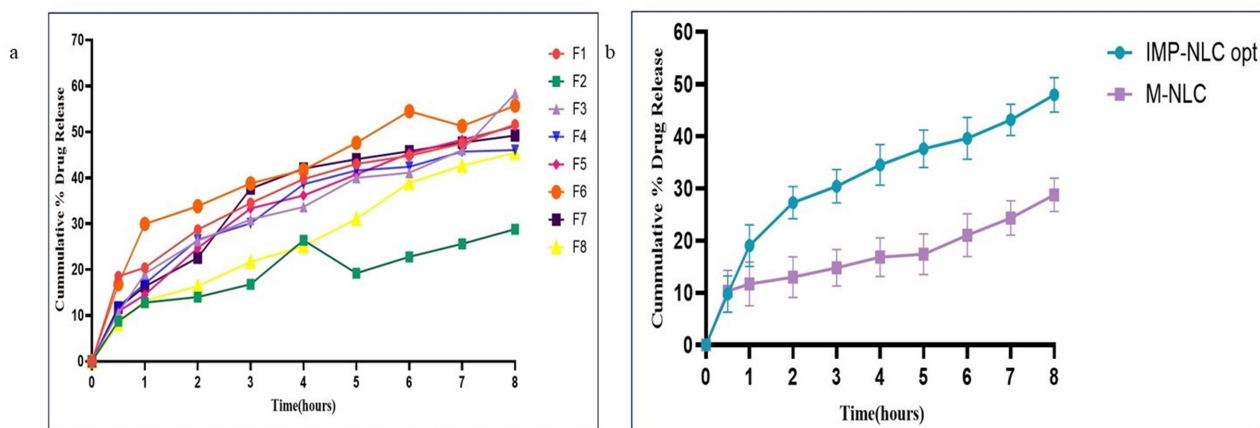


**Figure 7:** The drug's *in vitro* release of a) Comparative-graph of eight NLC Formulation b) IMP- NLCs opt and M-NLCs formulation.

diameter of all formulations fell within the desired range. It is noteworthy that a size greater than 200 nm is reported to be necessary for phagocytic activity and in this study, all formulation particle sizes were found to be greater than 200 nm.<sup>16</sup> M-NLC demonstrates a larger particle size compared to IMP-NLC opt, indicating that mannosylation has significantly increased particle diameter. This could be attributed to the acidic environment facilitating mannose ring opening and subsequent reaction with the aldehyde group and amine on the NLC surface. Both IMP-NLC opt and M-NLC exhibited a PDI<0.5, indicating homogeneous particle dispersion. The zeta potential of the formulation indicates electrostatic repulsion within the colloidal dispersion and shows a negative charge, attributed to the use of anionic lipids such as oleic acid. The zeta potential was found to be increase for M-NLCs compared to IMP-NLCs opt, indicating an increase in stability due to mannosylation. The FTIR studies of physical mixtures retained all the important functional groups of the drug and excipient. The spectra showed no new peaks, confirming the drug's compatible with the excipients. The M-NLC spectra indicated the synthesis of Schiff's base, suggesting mannose ring opening and the interaction of the aldehyde (CHO) group with the amine group present on the Nanostructured Carrier (NLC).<sup>17</sup> The entrapment efficiency for IMP-NLC opt and M-NLC does much difference which mannosylation does show any difficulty in drug encapsulation with mannose-coating. The surface morphology was analyzed using phase contrast microscopy and Atomic Force Microscopy (AFM). The phase- contrast images and AFM images shows the particle were spherical in shape. The *in vitro* drug release pattern, as already mentioned, exhibits a dual-release pattern. The early rapid drug liberation might be the dispersion of drug on the lipid core outer surface, succeeded by a gradual and steady release., either through erosion of the lipid core or by diffusion. This is in agreement with a previously reported study.<sup>18</sup> When compared to IMP-NLC opt, the formulation containing M-NLC shows a slower release at the end of 8 hr. This might be related to the existence of a mannose layer on the outermost layer of the lipid carrier, which contributes to its slowed release.<sup>19</sup>

The drug release kinetics were analyzed using mathematical models, revealing a Weibull release model for IMP-NLC and a Korsmeyer-Peppas model for M-NLC. The release kinetics aid in gaining insights into the drug release mechanism and further studying the pharmacokinetic behaviour of the drug encapsulated in NLCs core.

## CONCLUSION

In this study, nano-structured lipid carriers loaded with imipramine were fabricated employing the homogenization method. The optimized formulation was efficiently developed using a 2<sup>3</sup>-factorial design, considering all factors and the responses were evaluated statistically. Parameters such as Particle Size (PS), PDI, zeta potential, shape, encapsulation efficiency, *in vitro* drug release and kinetics were determined and compared between IMP-NLC opt and M-NLC. The results showed uniform particle size distribution and good entrapment. The drug release resembled a dual pattern, with a progressive and longer release over time. Further *in vitro* cell line studies and cytotoxicity assessments of both IMP-NLC and M-NLC against leishmaniasis may help determine their leishmanicidal activity.

## ACKNOWLEDGEMENT

The authors express their gratitude to PSG College of Pharmacy affiliated to Dr. M.G.R University for providing essential facilities and ongoing support throughout the study.

## CONFLICT OF INTEREST

The authors declare that there is no conflict of interest.

## ABBREVIATIONS

UV: Ultraviolet; *n*: Release exponent; *R*<sup>2</sup>: Regression coefficient; IMP-NLC opt: Optimized Imipramine loaded nano lipid carrier; M-NLC: Mannosylated Imipramine loaded Nano lipid carrier; AFM: Atomic Force Microscopy; PS: Particle size;



**PDI:** Polydispersity Index; **FTIR:** Fourier Transform Infrared Spectroscopy.

## REFERENCES

1. Wang Q, Cheng H, Zhou K, Wang L, Dong S, Wang D, *et al.* Nanostructured lipid carriers as a delivery system of biochanin A. *Drug Deliv.* 2013;20(8):331-7. doi: 10.3109/10717544.2013.838716, PMID 24111887.
2. Weber S, Zimmer A, Pardeike J. Solid lipid nanoparticles (SLN) and nanostructured lipid carriers (NLC) for pulmonary application: a review of the state of the art. *Eur J Pharm Biopharm.* 2014;86(1):7-22. doi: 10.1016/j.ejpb.2013.08.013, PMID 24007657.
3. Iqbal MA, Md S, Sahni JK, Baboota S, Dang S, Ali J. Nanostructured lipid carriers' system: recent advances in drug delivery. *J Drug Target.* 2012;20(10):813-30. doi: 10.3109/1061186X.2012.716845, PMID 22931500.
4. Serafim TD, Coutinho-Abreu IV, Oliveira F, Meneses C, Kamhawi S, Valenzuela JG. Sequential blood meals promote *Leishmania* replication and reverse metacyclogenesis augmenting vector infectivity. *Nat Microbiol.* 2018;3(5):548-55. doi: 10.1038/s41564-018-0125-7, PMID 29556108.
5. Scott P, Novais FO. Cutaneous leishmaniasis: immune responses in protection and pathogenesis. *Nat Rev Immunol.* 2016;16(9):581-92. doi: 10.1038/nri.2016.72, PMID 27424773.
6. Kunjachan S, Gupta S, Dwivedi AK, Dube A, Chourasia MK. Chitosan-based macrophage-mediated drug targeting for the treatment of experimental visceral leishmaniasis. *J Microencapsul.* 2011;28(4):301-10. doi: 10.3109/02652048.2011.559281, PMID 21545321.
7. Mukherjee S, Pradhan S, Ghosh S, Sundar S, Das S, Mukherjee B, *et al.* Short-course treatment with imipramine entrapped in squalene liposomes results in sterile cure of experimental visceral leishmaniasis induced by antimony resistant *Leishmania donovani* with increased efficacy. *Front Cell Infect Microbiol.* 2020;10:595415. doi: 10.3389/fcimb.2020.595415, PMID 33240825.
8. Gupta MK, Sansare V, Shrivastava B, Jadhav S, Gurav P. Fabrication and evaluation of mannose decorated curcumin loaded nanostructured lipid carriers for hepatocyte targeting: *in vivo* hepatoprotective activity in Wistar rats. *Curr Res Pharmacol Drug Discov.* 2022;3:100083. doi: 10.1016/j.crphar.2022.100083, PMID 35118372.
9. Pinheiro M, Ribeiro R, Vieira A, Andrade F, Reis S. Design of a nanostructured lipid carrier intended to improve the treatment of tuberculosis. *Drug Des Dev Ther.* 2016;10:2467-75. doi: 10.2147/DDDT.S104395, PMID 27536067.
10. Jain A, Agarwal A, Majumder S, Lariya N, Khaya A, Agrawal H, *et al.* Mannosylated solid lipid nanoparticles as vectors for site-specific delivery of an anti-cancer drug. *J Control Release.* 2010;148(3):359-67. doi: 10.1016/j.jconrel.2010.09.003, PMID 20854859.
11. Costa A, Sarmento B, Seabra V. Mannose-functionalized solid lipid nanoparticles are effective in targeting alveolar macrophages. *Eur J Pharm Sci.* 2018;114:103-13. doi: 10.1016/j.ejps.2017.12.006, PMID 29229273.
12. Rebouças-Silva J, Tadini MC, Devequi-Nunes D, Mansur AL, S Silveira-Mattos P, I de Oliveira C, *et al.* Evaluation of *in vitro* and *in vivo* efficacy of a novel amphotericin B-loaded nanostructured lipid carrier in the treatment of *Leishmania braziliensis* infection. *Int J Nanomedicine.* 2020;15:8659-72. doi: 10.2147/IJN.S262642, PMID 33177824.
13. Ameduzzafar QM, Qumber M, Alruwaili NK, Bukhari SN, Alharbi KS, Imam SS, *et al.* BBD-based development of itraconazole loaded nanostructured lipid carrier for topical delivery: *in vitro* evaluation and antimicrobial assessment. *J Pharm Innov.* 2021;16(1):85-98. doi: 10.1007/s12247-019-09420-5.
14. Souto EB, Mehnert W, Müller RH. Polymorphic behaviour of Compritol® 888 ATO as bulk lipid and as SLN and NLC. *J Microencapsul.* 2006;23(4):417-33. doi: 10.1080/02652040600612439, PMID 16854817.
15. Nagaich U, Gulati N. Nanostructured lipid carriers (NLC) based controlled release topical gel of clobetasol propionate: design and *in vivo* characterization. *Drug Deliv Transl Res.* 2016;6(3):289-98. doi: 10.1007/s13346-016-0291-1, PMID 27072979.
16. Kusumoputro S, Au C, Lam KH, Park N, Hyun A, Kusumoputro E, *et al.* Liver-targeting nanoplateforms for the induction of immune tolerance. *Nanomaterials (Basel).* 2023;14(1):67. doi: 10.3390/nano14010067, PMID 38202522.
17. Xavier DA, Srividhya N. Synthesis and study of Schiff base ligands. *IOSR JAC.* 2014;7(11):6-15. doi: 10.9790/5736-071110615.
18. Zhang K, Lv S, Li X, Feng Y, Li X, Liu L, *et al.* Preparation, characterization and *in vivo* pharmacokinetics of nanostructured lipid carriers loaded with oleanolic acid and gentiopicrin. *Int J Nanomedicine.* 2013;8:3227-39. doi: 10.2147/IJN.S45031, PMID 24009420.
19. Chowdhary SJ, Chowdhary A, Agrawal GP, Jain A. A formulation of paromomycin sulphate as a promising fucose-conjugated nanostructured lipid carrier for antileishmanial drug delivery. *ACS Biomater Sci Eng.* 2021;7(1):157-65. doi: 10.1021/acsbomaterials.0c01165, PMID 33350804.

**Cite this article:** Roy R, Sankar V, Ragavendra P. Formulation Development, Optimization and Evaluation of Imipramine Loaded Nano-Structured Lipid Carrier. *J Young Pharm.* 2024;16(3):547-55.